# An efficient technique based on barycentric interpolation collocation method for the time fractional Allen-Cahn equation

**Rong Huang, Zhifeng Weng**[*]

Fujian Province University Key Laboratory of Computation Science, School of Mathematical Sciences,
Huaqiao University, Quanzhou 362021 China

[*]Corresponding author, e-mail: zfwmath@hqu.edu.cn

**ABSTRACT**: This paper aims to numerically study two well-known difference formulas based on barycentric interpolation collocation method for the time fractional Allen-Cahn equation. The L1 formula and the fast convolution algorithm are used to approximate the Caputo time fractional derivative respectively, and the barycentric interpolation collocation method is applied to discretize the spatial derivative. Moreover, consistency analysis of semi-discretized in space and fully discretized nonlinear scheme is demonstrated. The nonlinear term is treated by explicit scheme to derive the discrete linear equations. Numerical experiments are presented to validate the theoretical results and show the configurations of phase field evolution.

**KEYWORDS**: time fractional Allen-Cahn equation, barycentric interpolation collocation, L1 scheme, fast evaluation

**MSC2020**: 65M70 65L20

## INTRODUCTION

The Allen-Cahn equation was originally introduced by Allen and Cahn [1] as a mathematical model for antiphase domain coarsening in a binary alloy. After that, Allen-Cahn equation has been widely applied to various problems such as image analysis [2, 3], crystal growth [4], phase transitions [5], and mean curvature flaws [6]. Compared with a large number of studies [7, 8] for the integer-order Allen-Cahn equation, there are very less numerical results on the fractional-order Allen-Cahn equations because the fractional derivative brings up expensive computational cost, while the fractional Allen-Cahn equation provides more comprehensive explanation of memory, genetics, nonlocality and path dependence involved in complex environments due to the historical dependence and nonlocality of fractional derivative. The time fractional Allen-Cahn equation has a wide range of application prospects, however, its analytical solution is often difficult or impossible to find. Therefore, it is one of the main topics for researchers. In this paper, we propose two schemes based on barycentric Lagrange interpolation collocation method for solving the time fractional Allen-Cahn (TFAC) equation with Dirichlet boundary condition, which may be written as

$$
{}^{C}_{0}D^{\alpha}_{t}u(\boldsymbol{x},t) = \epsilon^2 \Delta u(\boldsymbol{x},t) - F'(u(\boldsymbol{x},t)) \qquad (1)
$$

for $(\boldsymbol{x},t) \in \Omega \times (0,T]$, where the phase field function $u(\boldsymbol{x},t)$ represents the concentration function of the two metallic components of the alloy, $\epsilon$ is a positive constant as an interface width parameter, and $F(u) = (u^2-1)^2/4$ is bistable, $F'(u) = f(u) = u^3 - u$. $\Omega =$ $(a,b) \times (c,d)$ is a sufficiently smooth and bounded domain. The operator ${}^{C}_{0}D^{\alpha}_{t}$ represents the Caputo fractional derivative with the definition as following

$$
{}^{C}_{0}D^{\alpha}_{t}u(\boldsymbol{x},t) = \frac{1}{\Gamma(1-\alpha)} \int_0^t \frac{\partial_\sigma u(\boldsymbol{x},\sigma)}{(t-\sigma)^\alpha} \, \mathrm{d}\sigma \qquad (2)
$$

for $0 < \alpha < 1$, where $\Gamma(\cdot)$ stands for the gamma function.

Allen-Cahn equation can be viewed as the $L^2$-gradient flow with the following

$$
E(u(\boldsymbol{x},t)) = \int_\Omega \frac{\epsilon^2}{2} |\nabla u(\boldsymbol{x},t)|^2 + F(u(\boldsymbol{x},t)) \, \mathrm{d}\boldsymbol{x}. \qquad (3)
$$

By differentiating the energy $E(u)$ with respect to $t$, the TFAC equation is energy-decay, namely:

$$
\begin{aligned}
&{}^{C}_{0}D^{\alpha}_{t}E(u(\boldsymbol{x},t)) \\
&= \int_\Omega {}^{C}_{0}D^{\alpha}_{t}u(\boldsymbol{x},t)(-\epsilon^2 \Delta u(\boldsymbol{x},t) + F'(u(\boldsymbol{x},t))) \, \mathrm{d}\boldsymbol{x} \\
&= -\int_\Omega \left[ {}^{C}_{0}D^{\alpha}_{t}u(\boldsymbol{x},t) \right]^2 \, \mathrm{d}\boldsymbol{x} \leqslant 0 \qquad (4)
\end{aligned}
$$

Recently, the development of fractional-order operators has promoted the rapid development of the extension of the fractional-order Allen-Cahn equation, which has attracted more attention of many scholars. Consequently, many scholars have devoted themselves to the studies of various stable and efficient numerical simulation methods. Du et al [9] proposed a convex splitting scheme for the fractional Allen-Cahn equations. Liu et al [10] used a fast Caputo algorithm

combined with Fourier spectral method to solve the time fractional Allen-Cahn equation. Liao et al [11] presented a second-order nonuniform time-stepping scheme for the time fractional Allen-Cahn equation. Ji et al [12] presented two fast L1 time-stepping methods, including the backward Euler and stabilized semi-implicit schemes, for the time fractional Allen-Cahn equation. Hou et al [13] developed high-order efficient schemes based on L1 discretization and the extended scalar auxiliary variable approach for the time fractional Allen-Cahn equation. Quan et al [14] established the energy stability of high-order L2-type schemes for time-fractional phase-field equations; furthermore, a fractional energy law was established for the L2 implicit-explicit scheme. Jia et al [15] used the fractional backward difference formula (FBDF) combined with the spectral method to solve the fractional Allen-Cahn equation, and analyzed the error of the numerical format. Guo et al [16] used the novel adaptive Crank-Nicolson-type scheme to solve the time fractional Allen-Cahn equation. Wang et al [17] proposed a local discontinuous Galerkin method combined with nonuniform time discretizations for the time-fractional Allen-Cahn equation.

Compared to many works of TFAC equation depending on mesh partition, the barycentric interpolation collocation is a revolutionary meshless method. It has captured attention of scholars due to its high accuracy and ability to treat irregular domains. The barycentric interpolation formula is accurate highly, fast, stable and easy on program implementation, which was lately extended to solve various partial differential equations, including nonlinear parabolic partial differential equations [18], the optimal control problem [19], Sine-Gordon equation [20], high-dimensional Fredholm integral equation [21], integer-order Allen-Cahn equation [22], etc. Recently, Yi et al [23] presented the error analysis of the barycentric Lagrange interpolation collocation scheme. Li et al [24] adopted the barycentric interpolation collocation algorithm to solve the fractional differential equations, and error analysis of the Gauss quadrature formula with weights $\rho(\tau) = (t - \tau)^{(\xi - \alpha)}$ is provided.

The L1 difference scheme is a classical discretization method in time for the Caputo derivative, addressing a weak singularity difficulty at $t = 0$. In recent years, it has attracted the attention of numerous academics [26–30]. Tang et al [26] first proved the analysis of energy dissipation and numerical stability of time-fractional gradient flow equations. They applied the L1 scheme to the time-fractional derivative with treating other terms in an implicit way. In [27], a time-stepping L1 scheme for the sub-diffusion equation with a Riemann-Liouville time fractional derivative was developed and analyzed. Zhou and Stynes [28] proved the optimal convergence rate of L1 scheme for the time fractional initial-value problem.

To our knowledge, nobody uses barycentric interpolation collocation method for the time fractional Allen-Cahn equation. Based on the above works, we focus on two fully discrete schemes for the TFAC equation, which are L1 scheme and fast convolution algorithm in time combined with the barycentric interpolation collocation method in space. Moreover, we will give consistency analysis of the semi-discretized scheme in space and fully discretized nonlinear scheme.

## EFFICIENT NUMERICAL ALGORITHM

### Barycentric Lagrange interpolation collocation method

In this paper, a novel meshless method is presented to discretize TFAC equation in space. Suppose $M + 1$ distinct nodes $x_k$ $(k = 0, 1, \ldots, M)$ be given, together with a set of functional value $v_k$ at the discrete node $x_k$ correspondingly. Let $Q(x)$ denotes interpolation polynomial to be the approximate value of $v(x)$, satisfying $Q(x_k) = v_k$ $(k = 0, 1, \ldots, M)$.

According to the Weierstrass theorem, polynomial $Q(x)$ is unique, which can be rewritten in Lagrange interpolation polynomial form

$$v(x) \approx Q(x) = \sum_{k=0}^{M} L_k(x) v_k, \quad k = 0, 1, \ldots, M, \quad (5)$$

where $L_k(x)$ is the Lagrange basis function and

$$L_k(x) = \frac{\prod\limits_{i \neq k}^{M} (x - x_i)}{\prod\limits_{i \neq k}^{M} (x_k - x_i)}, \quad k = 0, 1, \ldots, M.$$

Define $L(x) = (x - x_0)(x - x_1) \cdots (x - x_M)$, thus the basis function $L_k(x)$ and $Q(x)$ can be expressed in another form

$$L_k(x) = L(x) \frac{\omega_k}{x - x_k}, \quad k = 0, 1, \ldots, M, \quad (6)$$

$$Q(x) = L(x) \sum_{k=0}^{M} \frac{\omega_k}{x - x_k} v_k, \quad (7)$$

where $\omega_k = 1 / \prod\limits_{k \neq i} (x_k - x_i)$ is the barycentric weighet.

Supposing $Q(x) = 1$, then replacing the assumption in the Eq. (7), it can be derived that

$$1 = L(x) \sum_{k=0}^{M} \frac{\omega_k}{x - x_k}. \quad (8)$$

The barycentric Lagrange interpolation formula for $v(x)$ can be expressed, with combining Eqs. (7)

and (8) and cancelling the common polynomial $L(x)$.

$$Q(x) = \frac{\sum_{k=0}^{M} \frac{\omega_k}{x-x_k} v_k}{\sum_{k=0}^{M} \frac{\omega_k}{x-x_k}} := \sum_{k=0}^{M} \psi_k(x) v_k, \qquad (9)$$

where

$$\psi_k(x) = \frac{\frac{\omega_k}{x-x_k}}{\sum_{k=0}^{M} \frac{\omega_k}{x-x_k}}.$$

The barycentric Lagrange interpolation formula has excellent numerical stability when selecting the Chebyshev points, so discrete nodes and corresponding barycentric weights are as follows

$$x_k = \cos\left(\frac{k}{M}\pi\right), \quad k = 0, 1, \ldots, M. \qquad (10)$$

$$\omega_k = (-1)^k \delta^k, \quad \delta^k = \begin{cases} \frac{1}{2}, & k = 0 \text{ or } M, \\ 1, & \text{else.} \end{cases} \qquad (11)$$

Thus, the $\mu$-order derivative of $Q(x)$ at the different node $x_i$ $(i = 0, 1, \ldots, M)$ can be obtained

$$Q^{(\mu)}(x_i) = \sum_{k=0}^{M} \psi_k^{(\mu)}(x_i) v_k := \sum_{k=0}^{M} D_{ik}^{(\mu)} v_k \qquad (12)$$

for $\mu = 1, 2, \ldots$, where $D_{ik}^{(\mu)} = \psi_k^{(\mu)}(x_i)$ denotes the element of the differentiation matrix $D^{(\mu)}$.

By Eqs. (9)–(12), we have [25]

$$\begin{cases} D_{ik}^{(1)} = \frac{w_k}{w_i} \frac{1}{(x_i-x_k)}, & i \neq k, \\ D_{ii}^{(1)} = -\sum_{k=0, k\neq i}^{M} D_{ik}^{(1)}, \end{cases} \qquad (13)$$

$$\begin{cases} D_{ik}^{(2)} = -2\frac{w_k}{w_i}\frac{1}{x_i-x_k}\sum_{j\neq i}\frac{w_j}{w_i}\frac{1}{x_i-x_j} + \frac{1}{x_i-x_k}, & i \neq k, \\ D_{ii}^{(2)} = -\sum_{k=0, k\neq i}^{M} D_{ik}^{(2)}. \end{cases} \qquad (14)$$

And the elements of the differentiation matrix $D^{(\mu)}$ can be calculated by mathematical induction method

$$\begin{cases} D_{ik}^{(\mu)} = \mu\left(D_{ii}^{(\mu-1)}D_{ik}^{(1)} - \frac{D_{ik}^{(\mu-1)}}{(x_i-x_k)}\right), & i \neq k, \\ D_{ii}^{(\mu)} = -\sum_{k=0, k\neq i}^{M} D_{ik}^{(\mu)}. \end{cases} \qquad (15)$$

**L1 difference scheme**

The L1 difference scheme is a classical discretization method in time for the Caputo-type fractional derivative, addressing a weak singularity difficulty at $t = 0$. Based on the L1 formula, we discretize TFAC equation in time direction in this paper. Firstly, we introduce a uniform mesh with the time size $\tau := t_s - t_{s-1} = T/N$,

$s = 1, 2, \ldots, N$. Thus, $_0^C D_t^\alpha u(x, t)$ at $t = t_{s+1}$ can be approximated by L1 discretization as follows

$$_0^C D_t^\alpha u(x, t_{s+1}) \approx \frac{1}{\Gamma(1-\alpha)} \sum_{j=1}^{s+1} \int_{t_{j-1}}^{t_j} \frac{\partial_p u(x, p)}{(t_{s+1}-p)^\alpha} \, \mathrm{d}p$$

$$= \frac{1}{\Gamma(1-\alpha)} \sum_{j=1}^{s+1} \frac{u(x, t_j) - u(x, t_{j-1})}{\tau} \int_{t_{j-1}}^{t_j} \frac{1}{(t_{s+1}-p)^\alpha} \, \mathrm{d}p + R^{s+1}$$

$$= \frac{\tau^{-\alpha}}{\Gamma(2-\alpha)} \sum_{j=1}^{s+1} b_{s+1-j}[u(x, t_j) - u(x, t_{j-1})] + R^{s+1}. \qquad (16)$$

where $b_j = (j+1)^{1-\alpha} - j^{1-\alpha}$, $0 \leq j \leq s$, and $R^{s+1}$ is the truncation error for the $(s+1)$-th step.

Consequently, the Caputo-type time fractional derivative is approximated by the following L1 scheme

$$\mathbb{D}_t^\alpha u^{s+1} \approx \frac{\tau^{-\alpha}}{\Gamma(2-\alpha)}\left[b_0 u^{s+1} - \sum_{j=1}^{s}(b_{s-j} - b_{s+1-j})u^j - b_s u^0\right]$$

$$:= \zeta(\tau, \alpha)\left[b_0 u^{s+1} - \sum_{j=1}^{s}(b_{s-j} - b_{s+1-j})u^j - b_s u^0\right], \qquad (17)$$

where $u^{s+1}$ is the approximation value of $u(x, t_{s+1})$ at the time node $t_{s+1}$, $\zeta(\tau, \alpha) = \tau^{-\alpha}/\Gamma(2-\alpha)$.

And a consistency and stability [29] bounds the truncation error in the computed solution $u^{s+1}$ by

$$|R^{s+1}| \leq C\tau^{2-\alpha}, \qquad (18)$$

where $C$ is a positive constant.

**Fast convolution algorithm**

In this subsection, a fast convolution algorithm [30] is proposed to save computing time and storage space caused by the memory dependence of the Caputo derivative. We can split the L1 scheme of Caputo derivative into the sum of two parts, including a history part and a local part, which are expressed by

$$_0^C D_t^\alpha u^{s+1} = \frac{1}{\Gamma(1-\alpha)} \int_0^{t_s} \frac{u'(x, p)}{(t_{s+1}-p)^\alpha} \, \mathrm{d}p$$

$$+ \frac{1}{\Gamma(1-\alpha)} \int_{t_s}^{t_{s+1}} \frac{u'(x, p)}{(t_{s+1}-p)^\alpha} \, \mathrm{d}p$$

$$:= C_h(t_{s+1}) + C_l(t_{s+1}), \qquad (19)$$

where the equality defines the history part $C_h(t_{s+1})$ and the local part $C_l(t_{s+1})$, respectively.

For the local part, we apply the standard L1 approximation. And the convolution integral of $u(t)$ with the kernel function $t^{-\alpha-1}$ is approximated by the sum-of-exponentials (SOE) approximation. Suppose a subinterval $[\Delta t, T] \in (0, T)$ is given, with an adequate small parameter $\varepsilon$ $(0 < \varepsilon \leq 1)$, there exist a set of positive values $s_i$ and positive weights $\omega_i$ $(i = 1, 2, \ldots)$ correspondingly, satisfying that

$$\left|\frac{1}{t^{\alpha+1}} - \sum_{i=1}^{N_{\exp}} \omega_i e^{-s_i t}\right| \leq \varepsilon, \qquad t \in [\Delta t, T], \qquad (20)$$

where $N_{\exp}$ represents the number of exponentials, which can be calculated by

$$N_{\exp} = O\left(\left(\log\frac{1}{\varepsilon}\right)\left(\log\frac{T}{\Delta t} + \log\log\frac{1}{\varepsilon}\right)\right.$$
$$\left. + \left(\log\frac{1}{\Delta t}\right)\left(\log\frac{1}{\Delta t} + \log\log\frac{1}{\varepsilon}\right)\right). \quad (21)$$

Thus, fast evaluation $\mathscr{F}_t^\alpha$ of L1 scheme can be included from (17)

$$\mathscr{F}_t^\alpha u^{s+1} = \zeta(\tau, \alpha)(u^{s+1} - u^s)$$
$$+ \frac{1}{\Gamma(1-\alpha)}\left[\frac{u^s}{\tau^\alpha} - \frac{u^0}{t_{s+1}^\alpha} - \alpha\sum_{i=1}^{N_{\exp}}\omega_i \Upsilon_i(t_{s+1})\right] \quad (22)$$

for $1 \leqslant s < N$, where $\Upsilon_i(t_{s+1}) = e^{(-s_i\Delta t)}\Upsilon_i(t_s) + \int_{t_{s-1}}^{t_s} e^{-s_i(t_{s+1}-\sigma)}u(\sigma)\,d\sigma$, $1 \leqslant s < N$, $\Upsilon_i(t_1) = 0$. Particularly, $\mathscr{F}_t^\alpha u^1 = \zeta(\tau, \alpha)(u^1 - u^0)$.

Let $^{\mathscr{F}}R^{s+1}u = {}_0^C D_t^\alpha u^{s+1} - \mathscr{F}_t^\alpha u^{s+1}$, the following lemma in [30] provides an error bound for the fast evaluation

$$\left|{}^{\mathscr{F}}R^{s+1}u\right| \leqslant \frac{\tau^{2-\alpha}}{\Gamma(2-\alpha)}\left(\frac{1-\alpha}{12} + \frac{2^{2-\alpha}}{2-\alpha} - (1+2^{-\alpha})\right)\max_{0\leqslant t\leqslant t_{s+1}}|u_{tt}|$$
$$+ \frac{\alpha\varepsilon t_s}{\Gamma(1-\alpha)}\max_{0\leqslant t\leqslant t_s}|u| \quad (23)$$

Compared with computational results, both fast evaluation and direct L1 scheme have the same error accuracy when $\varepsilon$ is sufficiently small. However, the memory requirement and computational cost of the fast algorithm are $O(N_{\exp})$ and $O(NN_{\exp})$, respectively, decreasing from $O(N)$ and $O(N^2)$, which demonstrates that the fast algorithm has obvious advantages.

## SEMI-DISCRETIZED SCHEME BASED ON BARYCENTRIC INTERPOLATION COLLOCATION METHOD

### Semi-discretized scheme in space for TFAC equation

In this section, we present efficient numerical algorithms to discretize the TFAC equation based on the BLIC method in space. First, the function $u(x, y, t)$ at the node $(x_k, y_l, t)$ can be written in the barycenter Lagrange interpolation formula

$$u(x, y, t) = \sum_{i=0}^M \sum_{j=0}^N \psi_i(x)\gamma_j(y)u(x_k, y_l, t) \quad (24)$$

for $0 \leqslant k \leqslant M$, $0 \leqslant l \leqslant N$.

Consider $u(x, y, t)$ to find the second-order partial derivatives of variables $x$ and $y$, respectively, namely

$$\begin{cases} u_{xx}(x, y, t) = \sum_{i=0}^M \sum_{j=0}^N \psi_i''(x)\gamma_j(y)u(x_k, y_l, t), \\ u_{yy}(x, y, t) = \sum_{i=0}^M \sum_{j=0}^N \psi_i(x)\gamma_j''(y)u(x_k, y_l, t), \end{cases} \quad (25)$$

where $\psi_k(x)$, $\gamma_j(y)$ are basis functions on the directions of $x$ and $y$.

Substituting Eqs. (23) and (24) into TFAC equation, implies that

$${}_0^C D_t^\alpha u(x_k, y_l, t) - \epsilon^2 \sum_{i=0}^M \sum_{j=0}^N \psi_i''(x)\gamma_j(y)u(x_k, y_l, t)$$
$$- \epsilon^2\sum_{i=0}^M \sum_{j=0}^N \psi_i(x)\gamma_j''(y)u(x_k, y_l, t) + f(u(x_k, y_l, t)) = 0 \quad (26)$$

with boundary conditions

$$u(x_0, y_l, t) = \chi_1(y_l, t), \quad u(x_M, y_l, t) = \chi_2(y_l, t),$$
$$u(x_k, y_0, t) = g_1(x_k, t), \quad u(x_k, y_N, t) = g_2(x_k, t),$$

for $l = 0, 1, \ldots, N$ and $k = 0, 1, \ldots, M$.

The semi-discretized scheme in space for the TFAC equation is derived by matrix form

$${}_0^C D_t^\alpha \mathbf{U}_h - \text{diag}(\epsilon^2)\left(C^{(2)}\otimes I_N + I_M\otimes D^{(2)}\right)\mathbf{U}_h + f(\mathbf{U}_h) = 0, \quad (27)$$

where $\mathbf{U}_h = [u_{00}(t), \ldots, u_{0N}(t), u_{10}(t), \ldots, u_{1N}(t), u_{M0}(t), \ldots, u_{MN}(t)]^T$, and $\otimes$ is kronecker product of matrix.

### Consistency analysis of semi-discretized scheme

In this section, we present consistency estimates of the semi-discretized scheme based on approximation properties of the barycentric Lagrange interpolation. For unknown function $u(x, y)$, the corresponding barycentric Lagrange interpolation function is $u_h(x, y)$, and the error $\zeta(x, y)$ holds the following definition

$$\zeta(x, y) = u(x, y) - u_h(x, y) \quad (28)$$

The approximation properties of the barycentric Lagrange interpolation have been presented in [23] as follow

**Lemma 1** *If* $u(x, y) \in C^{(n+1)}(\Omega)$, $\Omega = [a, b] \times [c, d]$ *is smooth and bounded domain, holds*

$$\begin{cases} \max|\zeta(x, y)| \leqslant \|u^{(n+1)}\|_\infty\left(c_x(\frac{eL_x}{2M})^M + c_y(\frac{eL_y}{2N})^N\right), \\ \max|\frac{\partial^2\zeta(x,y)}{\partial x^2}| \leqslant \|u^{(n+1)}\|_\infty\left(c_x(\frac{eL_x}{2(M-2)})^{M-2} + c_y(\frac{eL_y}{2N})^N\right), \\ \max|\frac{\partial^2\zeta(x,y)}{\partial y^2}| \leqslant \|u^{(n+1)}\|_\infty\left(c_x(\frac{eL_x}{2M})^M + c_y(\frac{eL_y}{2(N-2)})^{N-2}\right), \end{cases}$$

*where* $L_x = \frac{b-a}{2}$, $L_y = \frac{d-c}{2}$, $c_x$ *and* $c_y$ *are positive constants.*

Suppose $u(x_k, y_l, t)$ is the corresponding barycentric Lagrange interpolation of $u(x, y, t)$, and differential operator $\mathscr{G}$ holds the property

$$\mathscr{G}u(x, y, t) := {}_0^C D_t^\alpha u(x, y, t) - \epsilon^2 \Delta u(x, y, t)$$
$$+ f(u(x, y, t)) = 0. \quad (29)$$

$$\mathscr{G}u(x_k,y_l,t) := {}_0^C D_t^\alpha u(x_k,y_l,t) - \epsilon^2 \Delta u(x_k,y_l,t)$$
$$+ f(u(x_k,y_l,t)) = 0. \quad (30)$$

and

$$\lim_{(k,l)\to\infty} \mathscr{G}u(x_k,y_l,t) = 0. \quad (31)$$

Next, we will give the consistency analysis of spatial semi-discrete collocation schemes.

**Theorem 1** *If $u(x,y,t) \in C^{(n+1)}(\Omega) \times C^2(0,T]$, $\Omega = [a,b] \times [c,d]$, and $u(x_k,y_l,t)$ is the corresponding barycentric Lagrange interpolation of $u(x,y,t)$ and the nonlinear term $f(u)$ satisfies the Lipschitz condition, we have*

$$\max|u(x,y,t) - u(x_k,y_l,t)|$$
$$\leqslant C \|u^{(n+1)}\|_\infty \left( \left(\frac{eL_x}{2(M-2)}\right)^{M-2} + \left(\frac{eL_y}{2(N-2)}\right)^{N-2} \right), \quad (32)$$

*where $C$, $C_i$ ($i = 1,2,3,4$), $C_{11}$, $C_{12}$ are positive constants. $L_x = \frac{b-a}{2}$, $L_y = \frac{d-c}{2}$, $M+1$, $N+1$ are nodes of $x$ and $y$ directions.*

*Proof*: Combining Eqs. (29) and (30), we have

$$\mathscr{G}u(x,y,t) - \mathscr{G}u(x_k,y_l,t) = {}_0^C D_t^\alpha [u(x,y,t) - u(x_k,y_l,t)]$$
$$- \epsilon^2 [u_{xx}(x,y,t) - u_{xx}(x_k,y_l,t)]$$
$$- \epsilon^2 [u_{yy}(x,y,t) - u_{yy}(x_k,y_l,t)]$$
$$+ f(u(x,y,t)) - f(u(x_k,y_l,t))$$
$$:= \eta_1 + \eta_2 + \eta_3 + \eta_4, \quad (33)$$

where

$$\eta_1 := {}_0^C D_t^\alpha [u(x,y,t) - u(x_k,y_l,t)],$$
$$\eta_2 := -\epsilon^2 [u_{xx}(x,y,t) - u_{xx}(x_k,y_l,t)],$$
$$\eta_3 := -\epsilon^2 [u_{yy}(x,y,t) - u_{yy}(x_k,y_l,t)], \quad (34)$$
$$\eta_4 := f(u(x,y,t)) - f(u(x_k,y_l,t)).$$

According to the definition (2), using integration by parts and applying Lemma 1, we obtain

$$|\eta_1| \leqslant \left| \frac{t^{1-\alpha}}{\Gamma(2-\alpha)} [u_t(x,y,t) - u_t(x_k,y_l,t)] \right|$$
$$+ \left| \frac{1}{\Gamma(1-\alpha)} \int_0^t \frac{(t-\sigma)^{1-\alpha}}{1-\alpha} [u_{tt}(x,y,\sigma) - u_{tt}(x_k,y_l,\sigma)] d\sigma \right|$$
$$\leqslant \left| \frac{t^{1-\alpha}}{\Gamma(2-\alpha)} [u_t(x,y,t) - u_t(x_k,y_l,t)] \right|$$
$$+ \left| \frac{1}{\Gamma(1-\alpha)} \frac{t^{2-\alpha}}{\alpha-2} [u_{tt}(x,y,\varsigma) - u_{tt}(x_k,y_l,\varsigma)] \right|$$
$$\leqslant (C_{11}\|u_t\|_\infty + C_{12}\|u_{tt}\|_\infty) \|u^{(n+1)}\|_\infty \left( \left(\frac{eL_x}{2M}\right)^M + \left(\frac{eL_y}{2N}\right)^N \right)$$
$$\leqslant C_1 \|u^{(n+1)}\|_\infty \left( \left(\frac{eL_x}{2M}\right)^M + \left(\frac{eL_y}{2N}\right)^N \right). \quad (35)$$

$$|\eta_2| = \epsilon^2 \big| u_{xx}(x,y,t) - u_{xx}(x,y,t)$$
$$+ u_{xx}(x,y,t) - u_{xx}(x_k,y_l,t) \big|$$
$$\leqslant C_2 \|u^{(n+1)}\|_\infty \left( \left(\frac{eL_x}{2(M-2)}\right)^{M-2} + \left(\frac{eL_y}{2N}\right)^N \right). \quad (36)$$

$$|\eta_3| = \epsilon^2 \big| u_{yy}(x,y,t) - u_{yy}(x,y_l,t)$$
$$+ u_{yy}(x,y_l,t) - u_{yy}(x_k,y_l,t) \big|$$
$$\leqslant C_3 \|u^{(n+1)}\|_\infty \left( \left(\frac{eL_x}{2M}\right)^M + \left(\frac{eL_y}{2(N-2)}\right)^{N-2} \right). \quad (37)$$

As $f(u)$ satisfies the Lipschitz condition, we can suppose there exists a positive constant $K$, which holds

$$|\eta_4| = |f(u(x,y,t)) - f(u(x_k,y_l,t))|$$
$$\leqslant K |u(x,y,t) - u(x_k,y_l,t)|$$
$$\leqslant C_4 \|u^{(n+1)}\|_\infty \left( \left(\frac{eL_x}{2M}\right)^M + \left(\frac{eL_y}{2N}\right)^N \right). \quad (38)$$

Substituting (35)–(38) into (33), the proof completed. □

## FULLY DISCRETIZED SCHEME

In this part, we will establish fully discretized schemes of problem (1) by discretizing the temporal direction with L1 scheme. First, apply L1 scheme to discretize the ${}_0^C D_t^\alpha \mathbf{U}_h$ of Eq. (27) at time node $t_{s+1}$

$$\zeta(\tau,\alpha) \left[ b_0 \mathbf{U}_h^{s+1} - \sum_{j=1}^s (b_{s-j} - b_{s+1-j}) \mathbf{U}_h^j - b_s \mathbf{U}_h^0 \right]$$
$$- \text{diag}(\epsilon^2)(\mathbf{C}^{(2)} \otimes \mathbf{I}_N + \mathbf{I}_M \otimes \mathbf{D}^{(2)}) \mathbf{U}_h^{s+1} + f(\mathbf{U}_h^{s+1}) = 0. \quad (39)$$

Next, we will give the consistency analysis of fully discrete nonlinear scheme.

**Theorem 2** *If $u(x,y,t) \in C^{(n+1)}(\Omega) \times C^2(0,T]$, $\Omega = [a,b] \times [c,d]$, and $u(x_k,y_l,t_s)$ is the corresponding numerical solution of $u(x,y,t)$ and the nonlinear term $f(u)$ satisfies the Lipschitz condition, we have*

$$|u(x,y,t) - u(x_k,y_l,t_s)| \leqslant$$
$$\tilde{C}\left( \tau^{2-\alpha} + \|u^{(n+1)}\|_\infty \left( \left(\frac{eL_x}{2(M-2)}\right)^{M-2} + \left(\frac{eL_y}{2(N-2)}\right)^{N-2} \right) \right), \quad (40)$$

*where $\tilde{C}$ is a positive constant.*

*Proof*: Let $u(x,y,t_s)$ be the corresponding numerical solution of $u(x,y,t)$ solved by L1 scheme in time, we obtain

$${}_0^C \mathbb{D}_t^\alpha u(x,y,t_s) - \epsilon^2 \Delta u(x,y,t_s) + f(u(x,y,t_s)) = R^s, \quad (41)$$

where $R^s$ is the truncation error in time direction.

Combine Eq. (1) with Eq. (41), we obtain the following result based on the truncation error bound for the L1 scheme from (18)

$$\left| {}_0^C D_t^\alpha u(x,y,t) - {}_0^C \mathbb{D}_t^\alpha u(x,y,t_s) \right| = |R^s| \leqslant C\tau^{2-\alpha}. \quad (42)$$

Eq. (41) is discretized by BLIC scheme in space, and suppose $u(x_k, y_l, t_s)$ is the numerical solution of $u(x, y, t_s)$ based on the BLIC method, it holds

$$
{}^C_0\mathbb{D}^\alpha_t u(x_k, y_l, t_s) - \epsilon^2 \Delta u(x_k, y_l, t_s) + f(u(x_k, y_l, t_s))
$$
$$
= R^s + \eta^{k,l}, \quad (43)
$$

where $\eta^{k,l}$ is the truncation error in space.

Combine Eq. (41) with Eq. (43), we have

$$
{}^C_0\mathbb{D}^\alpha_t[u(x, y, t_s) - (u(x_k, y_l, t_s)]
$$
$$
- \epsilon^2[\Delta u(x, y, t_s) - \Delta u(x_k, y_l, t_s)]
$$
$$
+ [f(u(x, y, t_s)) - f(u(x_k, y_l, t_s))] = -\eta^{k,l}. \quad (44)
$$

From (44) and using similar techniques in Theorem 2 based on the nonlinear term which satisfies the Lipschitz condition, we can obtain

$$
|\eta^{k,l}| \leqslant \bar{C}\|u^{(n+1)}\|_\infty \left(\left(\frac{eL_x}{2(M-2)}\right)^{M-2} + \left(\frac{eL_y}{2(N-2)}\right)^{N-2}\right). \quad (45)
$$

According to (42) and (45), the consistency analysis of fully discrete nonlinear scheme can be derived

$$
|u(x, y, t) - u(x_k, y_l, t_s)| \leqslant \tilde{C}\left(\tau^{2-\alpha} + \right.
$$
$$
\left. \|u^{(n+1)}\|_\infty \left(\left(\frac{eL_x}{2(M-2)}\right)^{M-2} + \left(\frac{eL_y}{2(N-2)}\right)^{N-2}\right)\right). \quad (46)
$$
$$
\square
$$

The nonlinear term is treated by explicit scheme with the second order stabilized term to derive fully discrete scheme:

$$
\zeta(\tau, \alpha)\left[b_0\mathbf{U}_h^{s+1} - \sum_{j=1}^s (b_{s-j} - b_{s+1-j})\mathbf{U}_h^j - b_s\mathbf{U}_h^0\right]
$$
$$
- \mathrm{diag}(\epsilon^2) \cdot (\mathbf{C}^{(2)} \otimes \mathbf{I}_N + \mathbf{I}_M \otimes \mathbf{D}^{(2)})\mathbf{U}_h^{s+1}
$$
$$
+ f(\tilde{\mathbf{U}}_h^s) + \kappa\tau(\mathbf{U}_h^{s+1} - \mathbf{U}_h^s) = 0, \quad (47)
$$

where $\tilde{\mathbf{U}}_h^s = 2\mathbf{U}_h^s - \mathbf{U}_h^{s-1}$. In particular, the first-order form is used to solve $\tilde{\mathbf{U}}_h^1$ when $s = 0$. $\kappa$ is a stabilized parameter.

By arranging the Eq. (47) and defining $\lambda = \zeta(\tau, \alpha)b_0 + \kappa\tau$, we obtain DI-BLIC scheme:

$$
\left[\lambda\mathbf{I} - \mathrm{diag}(\epsilon^2) \cdot (\mathbf{C}^{(2)} \otimes \mathbf{I}_N + \mathbf{I}_M \otimes \mathbf{D}^{(2)})\right]\mathbf{U}_h^{s+1} =
$$
$$
\zeta(\tau, \alpha)\sum_{j=1}^s (b_{s-j} - b_{s+1-j})\mathbf{U}_h^j + \kappa\tau\mathbf{U}_h^s
$$
$$
- f(\tilde{\mathbf{U}}_h^s) + \zeta(\tau, \alpha)b_s\mathbf{U}_h^0, \quad s = 0, 1, \ldots, K. \quad (48)
$$

Similarly, we construct a fast numerical algorithm based on fast evaluation (22) in time named FDI-BLIC scheme:

$$
\left[\zeta(\tau, \alpha)\mathbf{I} - \mathrm{diag}(\epsilon^2) \cdot (\mathbf{C}^{(2)} \otimes \mathbf{I}_N + \mathbf{I}_M \otimes \mathbf{D}^{(2)}) + \kappa\tau\mathbf{I}\right]\mathbf{U}_h^{s+1}
$$
$$
- \frac{\alpha}{\Gamma(1-\alpha)}\sum_{i=1}^{N_{exp}} \omega_i \Upsilon_i(t_{s+1}) = \left[\zeta(\tau, \alpha) + \kappa\tau + \frac{1}{\Gamma(1-\alpha)\tau^\alpha}\right]\mathbf{U}_h^s
$$
$$
- f(\tilde{\mathbf{U}}_h^s) + \frac{1}{\Gamma(1-\alpha)t_{s+1}^\alpha}\mathbf{U}_h^0, \quad s = 0, 1, \ldots, K. \quad (49)
$$

## NUMERICAL EXPERIMENTS

In this section, we present several numerical examples to demonstrate the accuracy and stability of the proposed method. For convenience, some definitions are given

$$
E_\infty = \frac{\|U_h - U_e\|_\infty}{\|U_e\|_\infty},
$$
$$
\mathrm{Order} = \frac{\log(E_\infty(\tau_1)) - \log(E_\infty(\tau_1/2))}{\log(\tau_1) - \log(\tau_1/2)}, \quad (50)
$$

where $U_h$, $U_e$ denote numerical solutions and exact solutions, respectively, and $\|\cdot\|_\infty$ is the $L^\infty$ norm.

### Problem 1

This example is presented to verify the accuracy and convergence of proposed schemes. Considering on $[0, 1]^2 \times (0, T)$ with $\epsilon = 0.1$, $\kappa = 3$, $M = N = 12$, $T = 1$, the following time fractional Allen-Cahn equation is provided.

$$
{}^C_0 D^\alpha_t u - \epsilon^2 \Delta u + f(u) = G, \quad \text{in } \Omega \times [0, T],
$$
$$
u(x, y, 0) = u_0(x, y), \quad (x, y) \in \Omega, \quad (51)
$$
$$
u(x, y, t) = 0, \quad (x, y, t) \in \partial\Omega \times [0, T],
$$

where

$$
G(x, y, t) = \frac{\Gamma(6)}{\Gamma(6-\alpha)} t^{5-\alpha} \sin(\pi x)\sin(\pi y)
$$
$$
+ 2\epsilon^2\pi^2 t^5 \sin(\pi x)\sin(\pi y)
$$
$$
+ (t^5 \sin(\pi x)\sin(\pi y))^3 - t^5 \sin(\pi x)\sin(\pi y), \quad (52)
$$

and the exact solution is

$$
u(x, y, t) = t^5 \sin(\pi x)\sin(\pi y). \quad (53)
$$

The results are in Tables 1–3: with different fractional order $\alpha = 0.2, 0.5, 0.8$, both DI-BLIC and FDI-BLIC schemes for the time fractional Allen-Cahn equation have $2-\alpha$ temporal accuracy, which are consistent with theoretical convergence orders in time. In addition, the CPU time of FDI-BLIC scheme has significantly reduced compared with the DI-BLIC scheme.
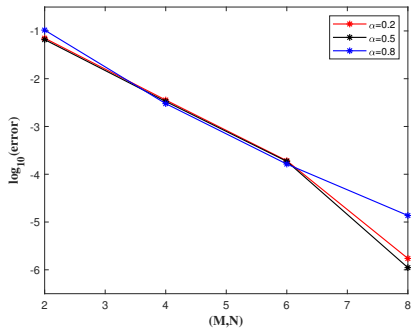
To test the convergence rate of different fractional order $\alpha$ in space, we choose above parameters with $\tau = 0.0001$, $\epsilon = 0.5$, and the computational results are presented in Fig. 1. One may see that convergence rates in space coincide with what we expected. The barycentric Lagrange collocation scheme has exponential convergence.

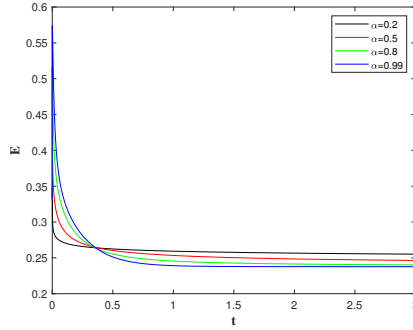**Table 1** Errors, convergence rates and computational time of $u$ solved by different schemes ($\alpha = 0.2$).

| $\tau$ | $E_\infty$ (DI-BLIC) | Order | Time | $E_\infty$ (FDI-BLIC) | Order | Time |
|---|---|---|---|---|---|---|
| 1/2500 | $9.9605 \times 10^{-7}$ | – | 57.05 | $9.9605 \times 10^{-7}$ | – | 34.88 |
| 1/5000 | $2.7967 \times 10^{-7}$ | 1.8325 | 132.09 | $2.7968 \times 10^{-7}$ | 1.8324 | 72.59 |
| 1/10000 | $7.8708 \times 10^{-8}$ | 1.8291 | 309.81 | $7.8691 \times 10^{-8}$ | 1.8295 | 164.25 |
| 1/20000 | $2.2201 \times 10^{-8}$ | 1.8259 | 890.63 | $2.2249 \times 10^{-8}$ | 1.8224 | 371.83 |

**Table 2** Errors, convergence rates and computational time of $u$ solved by different schemes ($\alpha = 0.5$).

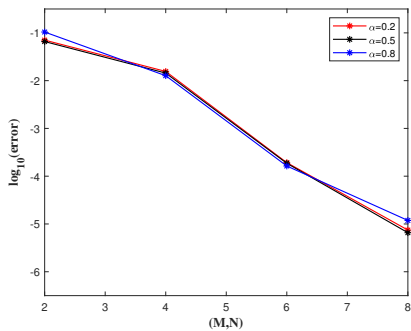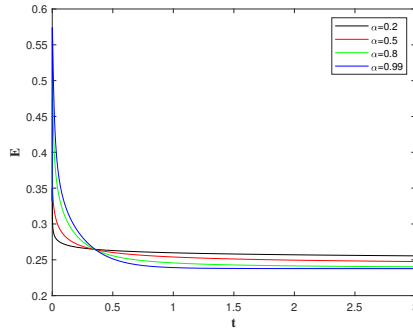| $\tau$ | $E_\infty$ (DI-BLIC) | Order | Time | $E_\infty$ (FDI-BLIC) | Order | Time |
|---|---|---|---|---|---|---|
| 1/2500 | $1.4079 \times 10^{-5}$ | – | 61.36 | $1.4079 \times 10^{-5}$ | – | 34.88 |
| 1/5000 | $5.0320 \times 10^{-6}$ | 1.4843 | 142.89 | $5.0320 \times 10^{-6}$ | 1.4843 | 73.81 |
| 1/10000 | $1.7927 \times 10^{-6}$ | 1.4890 | 332.25 | $1.7927 \times 10^{-6}$ | 1.4890 | 159.70 |
| 1/20000 | $6.3748 \times 10^{-7}$ | 1.4917 | 915.05 | $6.3748 \times 10^{-7}$ | 1.4917 | 369.53 |



(a) DI-BLIC



(a) DI-BLIC



(b) FDI-BLIC



(b) FDI-BLIC

**Fig. 1** The convergence rates in space of different fractional rate $\alpha$ for Problem 1 ($\tau = 0.0001$).

**Fig. 2** The curve of energy $E$ with $\epsilon = 0.3$, $\kappa = 2$ at different time by for Problem 2.

**Table 3** Errors, convergence rates and computational time of $u$ solved by different schemes ($\alpha = 0.8$).

| $\tau$ | $E_\infty$ (DI-BLIC) | Order | Time | $E_\infty$ (FDI-BLIC) | Order | Time |
|---|---|---|---|---|---|---|
| 1/2500 | $1.9463 \times 10^{-4}$ | – | 56.41 | $1.9463 \times 10^{-4}$ | – | 34.09 |
| 1/5000 | $8.4888 \times 10^{-5}$ | 1.1971 | 133.48 | $8.4888 \times 10^{-5}$ | 1.1971 | 72.45 |
| 1/10000 | $3.6992 \times 10^{-5}$ | 1.1984 | 321.00 | $3.6992 \times 10^{-5}$ | 1.1984 | 159.70 |
| 1/20000 | $1.6112 \times 10^{-5}$ | 1.1991 | 1042.44 | $1.6112 \times 10^{-5}$ | 1.1991 | 386.58 |

**Problem 2**

In order to investigate time evolution of the energy for two-dimensional time fractional Allen-Cahn equation with initial condition, the numerical experiment is considered on $[0,1]^2 \times (0,3]$ with the initial condition

$$u_0(x,y) = \epsilon^2 \cos(\pi x)\cos(\pi y). \tag{54}$$

Parameters are as follows: $\epsilon = 0.3$, $\kappa = 2$, $M = N = 12$, $\tau = 0.0001$ and $\alpha = 0.2, 0.5, 0.8, 0.99$, respectively. In Fig. 2, the energy decay at all time with different fractional order $\alpha$, consistent with the energy dissipation law of problem (1) physically.

**Problem 3**

Considering the following initial condition:

$$u_0(x,y) = h_1(x,y)h_2(x,y), \tag{55}$$

where

$$h_1 = \begin{cases} \tanh(\frac{3}{\epsilon}((x-0.5)^2+(y-0.4)^2-(0.25)^2)), & x > 0.3, \\ \tanh(\frac{3}{\epsilon}((y-0.4)^2-(0.15)^2)), & -0.3 \leqslant x \leqslant 0.3, \\ \tanh(\frac{3}{\epsilon}((x+0.5)^2+(y-0.4)^2-(0.25)^2)), & x < -0.3. \end{cases}$$

$$h_2 = \begin{cases} \tanh(\frac{3}{\epsilon}(x^2+(y-0.6)^2-(0.25)^2)), & y > 0.4, \\ \tanh(\frac{3}{\epsilon}(x^2-(0.15)^2)), & -0.4 \leqslant y \leqslant 0.4, \\ \tanh(\frac{3}{\epsilon}(x^2+(y+0.6)^2-(0.25)^2)), & y < -0.4. \end{cases}$$

We set the parameters $\Omega = [-1,1]^2 \times (0,15]$, $\epsilon = 0.08$, $\kappa = 2$, $M = N = 30$, $\tau = 0.001$ and $\alpha = 0.5, 0.7, 0.9$, respectively. Fig. 3 shows the interface shirking dynamics exists for different $\alpha$, for example, numerical solutions change from dumbbell shape, then evolving into an ellipse, merging into the small dot with the passage of time when $\alpha = 0.9$. Additionally, the shirking speed slows down significantly with the fractional order $\alpha$ decreasing.

**Problem 4**

Consider the following initial condition

$$u_0(x,y) = -\tanh\left(z(x,y)/\sqrt{2}\epsilon\right),$$
$$z(x,y) = \max\{z_1(x,y), z_2(x,y), z_3(x,y)\}, \tag{56}$$

where

$$z_1(x,y) = \sqrt{x^2+(y-2)^2} - 2 + 1.5\epsilon,$$
$$z_2(x,y) = \sqrt{x^2+y^2} - 1.5, \tag{57}$$
$$z_3(x,y) = \sqrt{x^2+(y+2)^2} - 2 + 1.5\epsilon.$$

By setting $\epsilon = 0.1$, $\kappa = 3$, $M = N = 40$, $\tau = 0.001$, $T = 15$, Fig. 4 shows that the equation appears coarsening phenomenon as time evolves with different fractional order $\alpha$. Obviously, the impact of the fractional order $\alpha$ on the interface evolution can be concluded when $\Omega = [-2,2]^2$, as $\alpha$ increases the coarsening dynamics becomes quick significantly, which is consistent with physical properties of fractional derivatives.
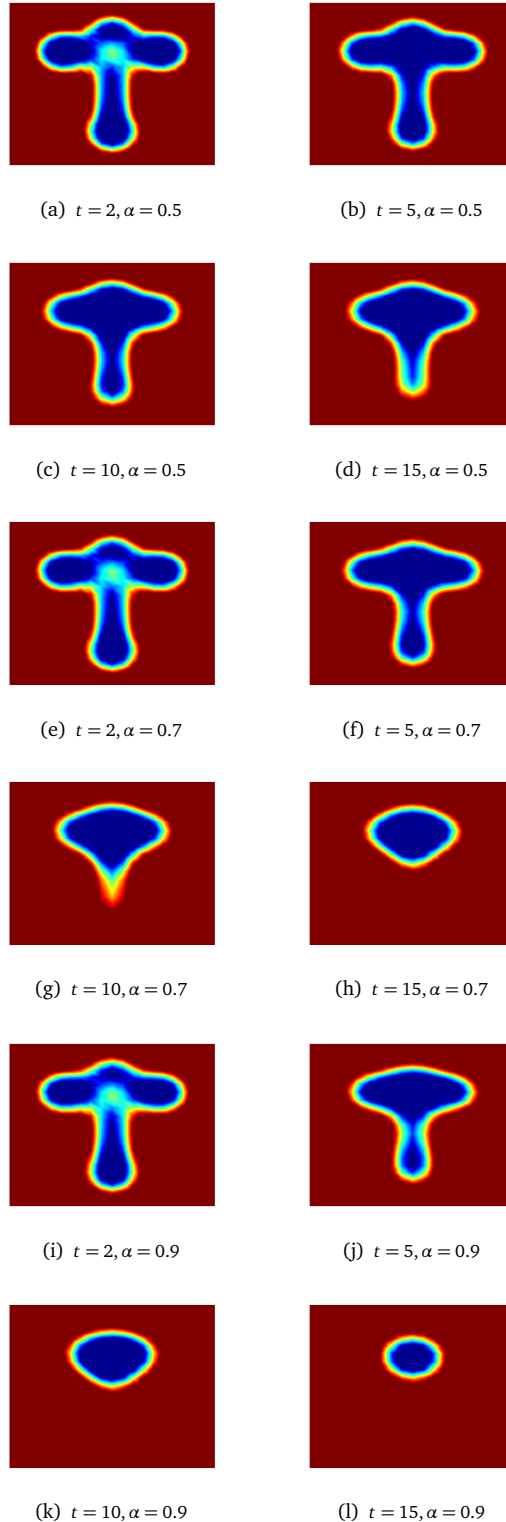


(a) $t = 2, \alpha = 0.5$  (b) $t = 5, \alpha = 0.5$

(c) $t = 10, \alpha = 0.5$  (d) $t = 15, \alpha = 0.5$

(e) $t = 2, \alpha = 0.7$  (f) $t = 5, \alpha = 0.7$

(g) $t = 10, \alpha = 0.7$  (h) $t = 15, \alpha = 0.7$

(i) $t = 2, \alpha = 0.9$  (j) $t = 5, \alpha = 0.9$

(k) $t = 10, \alpha = 0.9$  (l) $t = 15, \alpha = 0.9$

**Fig. 3** Snapshots of the numerical approximation of $u$ with different $\alpha$ at different time for Problem 3.

(a)  $t = 2, \alpha = 0.5$

(b)  $t = 6, \alpha = 0.5$

(c)  $t = 10, \alpha = 0.5$

(d)  $t = 15, \alpha = 0.5$

(e)  $t = 2, \alpha = 0.7$

(f)  $t = 6, \alpha = 0.7$

(g)  $t = 10, \alpha = 0.7$

(h)  $t = 15, \alpha = 0.7$

(i)  $t = 2, \alpha = 0.9$

(j)  $t = 6, \alpha = 0.9$

(k)  $t = 10, \alpha = 0.9$

(l)  $t = 15, \alpha = 0.9$

**Fig. 4** Snapshots of the numerical approximation of $u$ with different $\alpha$ at different time for Problem 4.

(a)  $t = 280, \alpha = 0.5$

(b)  $t = 300, \alpha = 0.5$

(c)  $t = 360, \alpha = 0.5$

(d)  $t = 400, \alpha = 0.5$

(e)  $t = 280, \alpha = 0.7$

(f)  $t = 300, \alpha = 0.7$

(g)  $t = 360, \alpha = 0.7$

(h)  $t = 400, \alpha = 0.7$

(i)  $t = 280, \alpha = 0.9$

(j)  $t = 300, \alpha = 0.9$

(k)  $t = 360, \alpha = 0.9$

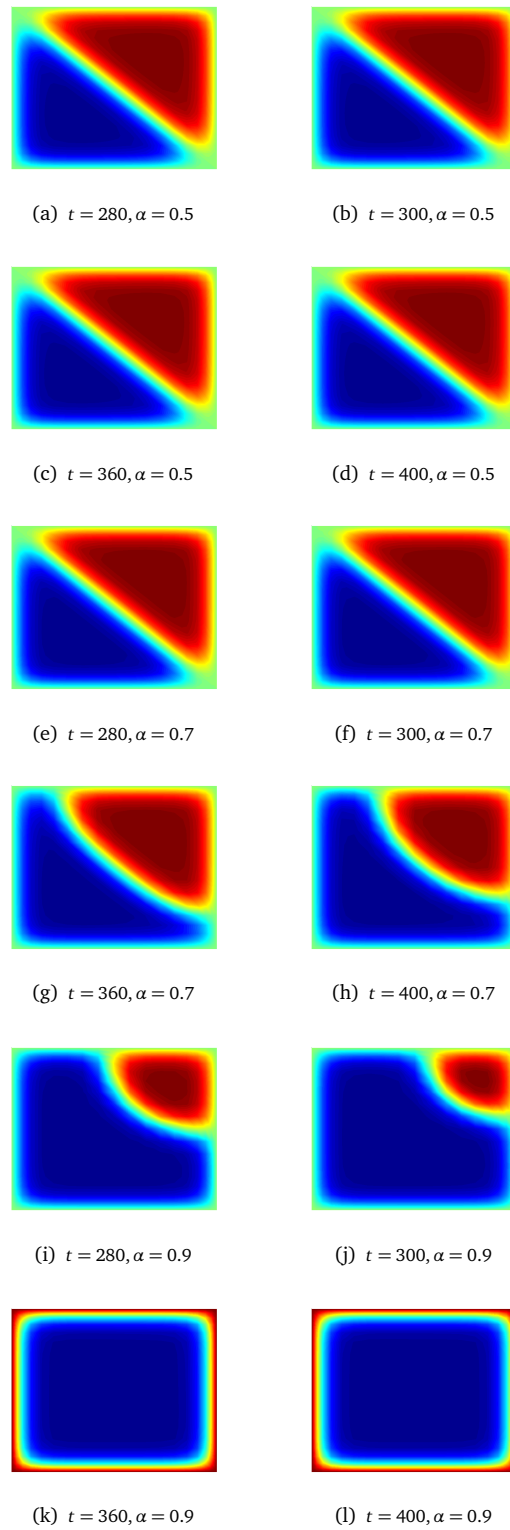(l)  $t = 400, \alpha = 0.9$
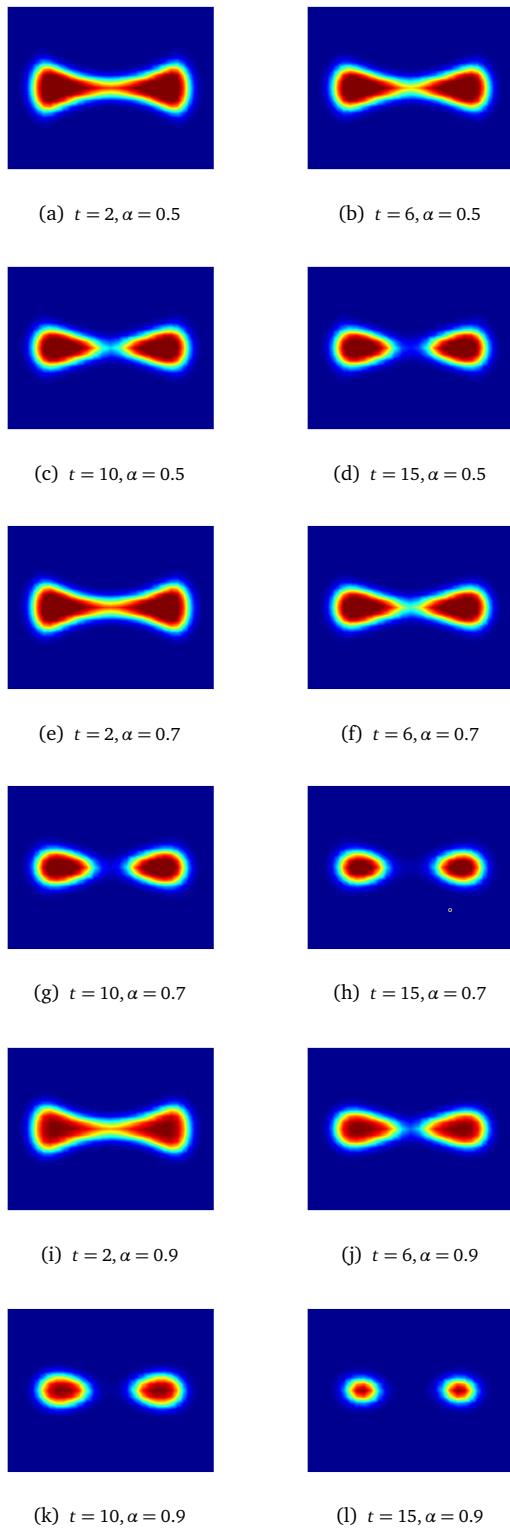
**Fig. 5** Snapshots of the numerical approximation of $u$ with different $\alpha$ at different time for Problem 5.

**Problem 5**

In this example, consider the following initial condition

$$u_0(x, y) = (x^2 - 1)(y^2 - 1)\sin(\pi x)\sin(\pi y). \quad (58)$$

We consider the TFAC equation on the computational domain $\Omega = [-1, 1]^2 \times (0, T]$ with zero Dirichlet boundary condition and set the parameters $\epsilon = 0.1$, $\kappa = 4$, $M = N = 20$, $T = 400$, $\tau = 0.01$, $\alpha = 0.5, 0.7, 0.9$, respectively.

Comparing snapshots of numerical approximation of $u$ for different fractional order $\alpha$ in Fig. 5, it can observed that coarsening phenomena of TFAC equation appears with the evolution of time. Moreover, the fractional order $\alpha$ can control the sharpness of the interface.

**CONCLUSION**

In this paper, combined with the L1 scheme and barycentric interpolation collocation method, a high order accurate numerical algorithm for the TFAC equation is developed, and a fast convolution evaluation is also developed to save computational cost. Furthermore, consistency analysis of semi-discretized and fully discrete nonlinear schemes have been presented. Numerical examples are demonstrated to validate the efficiency of the proposed method and show the configurations of phase field evolution. And the coarsening or shirking speed slows down when the fractional order decreases. The DI-BLIC and FDI-BLIC schemes have the same error accuracy when parameter $\varepsilon$ is sufficiently small. However, the fast convolution algorithm greatly reduces the computational cost compared with L1 difference formula, In the future, we will consider applying our numerical method to other time fractional nonlinear equations.

**REFERENCES**

1. Allen S, Cahn J (1979) A microscopic theory for antiphase boundary motion and its application to antiphase domain coarsening. *Acta Metall* **27**, 1085–1095.
2. Beneŝ M, Chalupecky V, Mikula K (2004) Geometrical image segmentation by the Allen-Cahn equation. *Appl Numer Math* **51**, 187–205.
3. Kay D, Tomasi A (2009) Color image segmentation by the vector valued Allen-Cahn phase-field model: A multigrid solution. *IEEE Trans Image Process* **18**, 2330–2339.
4. Kobayashi R (1993) Modeling and numerical simulations of dendritic crystal growty. *Physica D* **63**, 410–423.
5. Elliott C, Stinner B (2013) Computation of two-phase biomembranes with phase dependent material parameters using surface finite element. *Commun Comput Phys* **13**, 325–360.

6. Feng X, Prohl A (2003) Numerical analysis of the Allen-Cahn equation and approximation for mean curvature flaws. *Numer Math* **94**, 33–65.
7. Li H, Song Z, Hu J (2021) Numerical analysis of a second-order IPDGFE method for the Allen-Cahn equation and the curvature-driven geometric flow. *Comput Math Appl* **86**, 49–62.
8. Li J, Ju L, Cai Y, Feng X (2021) Unconditionally maximum bound principle preserving linear schemes for the conservative Allen-Cahn equation with nonlocal constraint. *J Sci Comput* **87**, 1–32.
9. Du Q, Yang J, Zhou Z (2020) Time-fractional Allen-Cahn equations: analysis and numerical methods. *J Sci Comput* **85**, 1–30.
10. Liu H, Cheng A, Wang H, Zhao J (2018) Time-fractional Allen-Cahn and Cahn-Hilliard phase-field models and their numerical investigation. *Comput Math Appl* **76**, 1876–1892.
11. Liao H, Tang T, Zhou T (2020) A second-order and nonuniform time-stepping maximum-principle preserving scheme for time-fractional Allen-Cahn equations. *J Comput Phys* **414**, 10947.
12. Ji B, Liao H, Zhang L (2020) Simple maximum-principle preserving time-stepping methods for time-fractional Allen-Cahn equation. *Adv Comput Math* **46**, 37.
13. Hou D, Zhu H, Xu C (2021) Highly efficient schemes for time-fractional Allen-Cahn equation using extended SAV approach. *Numer Algorithms* **88**, 1077–1108.
14. Quan C, Wang B (2022) Energy stable L2 schemes for time-fractional phase-field equations. *J Comput Phys* **458**, 111085.
15. Jia J, Zhang H, Xu H, Jiang X (2021) An efficient second order stabilized scheme for the two dimensional time fractional Allen-Cahn equation. *Appl Numer Math* **165**, 216–231.
16. Guo S, Ren J (2022) A novel adaptive Crank-Nicolson-type scheme for the time fractional Allen-Cahn model. *Appl Math Lett* **129**, 107943.
17. Wang Z, Sun L, Cao J (2022) Local discontinuous Galerkin method coupled with nonuniform time discretizations for solving the time-fractional Allen-Cahn equation. *Fractal Fract* **6**, 349.
18. Luo W, Huang T, Gu X, Liu Y (2017) Barycentric rational collocation methods for a class of nonlinear parabolic partial differential equations. *Appl Math Lett* **68**, 13–19.
19. Darehmiraki M, Rezazadeh A, Ahmadia A, Salahshour S (2022) An interpolation method for the optimal control problem governed by the elliptic convection-diffusion equation. *Numer Meth Part D E* **38**, 137–159.
20. Jiwari R (2021) Barycentric rational interpolation and local radial basis functions based numerical algorithms for multidimensional sine-Gordon equation. *Numer Meth Part D E* **37**, 1965–1992.
21. Liu H, Huang J, Zhang W, Ma Y (2019) Meshfree approach for solving multi-dimensional systems of Fredholm integral equations via barycentric Lagrange interpolation. *Appl Math Comput* **346**, 295–304.
22. Deng Y, Weng Z (2021) Barycentric interpolation collocation method based on Crank-Nicolson scheme for the Allen-Cahn equation. *AIMS Math* **6**, 3857–3873.
23. Yi S, Yao L (2019) A steady barycentric Lagrange interpolation method for the 2D higher-order time fractional telegraph equation with nonlocal boundary con-

dition with error analysis. *Numer Meth Part D E* **35**, 1694–1716.

24. Li J, Su X, Zhao K (2023) Barycentric interpolation collocation algorithm to solve fractional differential equations. *Math Comput Simulat* **205**, 340–367.

25. Klein G, Berrut J (2012) Linear rational finite differences from derivatives of barycentric rational interpolants. *SIAM J Numer Anal* **50**, 643–656.

26. Tang T, Yu H, Zhou T (2019) On energy dissipation theory and numerical stability for time-fractional phase-field equations. *SIAM J Sci Comput* **41**, A3757–A3778.

27. Mustapha K 2020) An L1 approximation for a fractional reaction-diffusion equation, a second-order error analysis over time-graded meshes. *SIAM J Numer Anal* **58**, 1319–1338.

28. Zhou Y, Stynes M (2022) Optimal convergence rates in time-fractional discretisations: the L1, $\overline{\text{L1}}$ and Alikhanov schemes. *E Asian J Appl Math* **12**, 503–520.

29. Gao G, Sun Z, Zhang H (2014) A new fractional numerical differentiation formula to approximate the Caputo fractional derivative and its applications. *J Comput Phys* **259**, 33–50.

30. Jiang S, Zhang J, Zhang Q, Zhang Z (2017) Fast evaluation of the Caputo fractional derivative and its applications to fractional diffusion equations. *Commun Comput Phys* **21**, 650–678.